# Do we have enough data? Robust reliability via uncertainty quantification

Roberto Rocchetta[a], Matteo Broggi[b], Edoardo Patelli[a,*]

[a] *Institute of Risk and Uncertainty, University of Liverpool, L69 3GQ, Liverpool, United Kingdom*
[b] *Institute for Risk and Reliability, Leibniz Hannover University, 30167 Hannover, Germany*

**Abstract**

A generalised probabilistic framework is proposed for reliability assessment and uncertainty quantification under a lack of data. The developed computational tool allows the effect of epistemic uncertainty to be quantified and has been applied to assess the reliability of an electronic circuit and a power transmission network. The strength and weakness of the proposed approach are illustrated by comparison to traditional probabilistic approaches. In the presence of both aleatory and epistemic uncertainty, classic probabilistic approaches may lead to misleading conclusions and a false sense of confidence which may not fully represent the quality of the available information. In contrast, generalised probabilistic approaches are versatile and powerful when linked to a computational tool that permits their applicability to realistic engineering problems.

*Keywords:* Uncertainty quantification, Information quality, Probability boxes, Dempster-Shafer, Computational tool, Reliability

## 1. Introduction

Nowadays it is generally well accepted that estimating the effect of uncertainty is a necessity, e.g. due to variation in parameters, operational conditions and in the modelling and simulations [1, 2]. In practical applications, situations are common where the analyst has to deal with poor quality data, few available specimens or inconsistent information. A typical example is a situation where very expensive samples have to be

*Corresponding author
*Email addresses:* Roberto.Rocchetta@liverpool.ac.uk (Roberto Rocchetta), broggi@bauinf.uni-hannover.de (Matteo Broggi), Edoardo.Patelli@liverpool.ac.uk (Edoardo Patelli)

collected, such as field proprieties of a deep reservoir [3] or performance of satellites [4]. In these cases, the amount of data will be scarce due to economic and time constraints and in several cases, expert elicitation (i.e. the best estimate of an expert) may be the only viable way of carrying on with the analysis [5].

As a consequence, strong assumptions may be needed to apply classical probabilistic methods given poor information quality, which can lead to erroneous reliability estimations and a false sense of confidence [6]. Generalised approaches, which fit in the framework of imprecise probability [6], are powerful methodologies for dealing with imprecise information and lack of data. These methodologies can be coupled to traditional probabilistic approaches in order to give a different prospective on the results, whilst avoiding the inclusion of unjustified assumptions and enhancing the overall robustness of the analysis. Generalised methods are rarely used in practice and this is probably due to lack of proper guidance, simulation tools, as well as some misconception in the interpretation of the results. Further comparison of different methodologies, both in theoretical aspects and in their applicability to real case studies, are required.

An original throughout analysis of the applicability of different methodologies to deal with different level of imprecision is presented. In addition, this paper presents a novel computational framework for generalised probabilistic analysis that can be adopted to deal with low quality data, few available samples and inconsistent information. Efficient and generally applicable computational strategies have been developed and implemented into OpenCossan [7]. The proposed framework is applied to assess the reliability of an electric series RLC circuit (a problem proposed by the NAFEMS Stochastics Working Group [8]) and of a power transmission network, both affected by a lack of data.

Generally speaking, different system performance indicators may be affected very differently by the same (lack of) data. The extent of a lack of information is not a-priori quantifiable and depends on the context of the analysis. The proposed approach is used to assess the information quality by comparison to classical probabilistic results and with respect to system reliability estimates. One of the main contributions of this work is a detailed comparison between classical and generalised probabilistic approaches from a straightforward applicative point of view and under different levels of imprecision. This serves as guidance for engineering practitioners to solve problems affected by a lack of data.

The rest of the paper is structured as follows: Section 2, presents the mathematical framework. In Section 3, a synthetic overview of the numerical framework and the proposed approach is proposed. The NAFEMS reliability problem is described and solved in Section 4. A lack of data problem for power network reliability estimation is solved in Section 5. A discussion on the limitations of the different approaches is presented in Section 6 and Section 7 closes the paper.

## 2. Mathematical Framework

Uncertainty is generally classified into two categories, aleatory and epistemic uncertainty. Aleatory uncertainty (Type I or irreducible uncertainty), represents stochastic behaviours and randomness of events and variables. Hence, due to its intrinsic random nature it is normally regarded as irreducible. Some examples of aleatory uncertainty are future weather conditions, stock market prices or chaotic phenomenon. Epistemic uncertainty (Type II or reducible uncertainty), is commonly associated with lack of knowledge about phenomena, imprecision in measurements and poorly designed models. It is considered to be reducible since further data can decrease the level of uncertainty, but this might not always be practical or feasible. In recent decades, efforts were focused on the explicit treatment of imprecise knowledge, non-consistent information and both epistemic and aleatory uncertainty. The methodologies are discussed in literature by different mathematical concepts: Evidence theory [9], interval probabilities [10], Fuzzy-based approaches [11], info-gap approaches [12] and Bayesian frameworks [13] are some of the most intensively applied concepts.
In this paper, Dempster-Shafer structures and probability boxes are used to model quantities affected by epistemic uncertainty, by aleatory uncertainty, or by a combination of the two. In addition, the Kolmogorov-Smirnov test [14] and Kernel Density Estimator [15] have been used to characterise the parameter uncertainty in case of small sample sizes.

### *2.1. Dempster-Shafer Structures and Probability Boxes*

The Dempster-Shafer (DS) theory is a well-suited framework to represent both aleatory and epistemic uncertainty. The difference between the axioms of classical probability theory and the DS theory is that the latter slacken the strict assumption of a

single probability measure for an event. It can be seen as a generalisation of Bayesian probability [16]. Mathematically, a Dempster-Shafer structure on the real line $\mathbb{R}$ can be identified with a basic probability assignment, that is a map as follows:

$$m : 2^{\mathbb{R}} \rightarrow [0, 1] \tag{1}$$

where the probability mass is $m([\underline{x}_i, \overline{x}_i]) = p_i$ for each focal element $[\underline{x}_i, \overline{x}_i] \subseteq \mathbb{R}$ with $i = 1, .., n$. $m(S)$ is equal 0 for the empty set $S = \emptyset$ and for $S \neq [\underline{x}_i, \overline{x}_i]$, such that $p_i > 0 \; \forall i$ and $\sum_i p_i = 1$. The upper bound on probability is referred as plausibility and the lower bound as belief, the cumulative plausibility function $Pl(x)$ and cumulative belief function $Bel(x)$ can be computed as $Pl(x) = \sum_{\underline{x}_i \leq x} m_i$ and $Bel(x) = \sum_{\overline{x}_i \leq x} m_i$. The continuous equivalents of DS structures are the so-called probability boxes or P-boxes. Mathematically, a P-box is a pair of lower and upper cumulative distribution functions $[\underline{F}_X, \overline{F}_X]$ from the possibility space $\Theta$ to [0,1] such that $\underline{F}_X(x) \leq \overline{F}_X(x) \; \forall \; x \in \Omega$ and $\Omega$ is a classical probability space. The upper and lower bounds for the CDFs are $\overline{F}_X = \overline{P}(X \leq x)$ and $\underline{F}_X = \underline{P}(X \leq x)$, respectively. Note that the probability distribution family associated with the random variable $x$ can be either specified or not specified. The former are generally named distributional P-boxes, or parametric P-boxes, the latter are named distribution-free P-boxes, or non-parametric P-boxes [13]. The wider the distance between the upper and the lower bound is, the higher the incertitude associated to the random variable. P-boxes and DS structures offer a straightforward way to deal with multiple and overlapping intervals, inconsistent sources of information and small sample sizes. The drawback is that the computational cost of propagating P-boxes and DS structures through the system is generally quite high, especially for a large number of intervals (i.e. focal elements) and time-consuming models. Nevertheless, the quantification approaches are generally not-intrusive and hence applicable to any model.

## 3. Generalised Probabilistic Reliability Analysis and Numerical Implementation

In modern engineering systems and critical infrastructures uncertainty quantification must be performed to assure an adequate level of safety and reliability. A broadly applied numerical approach, often used to deal with uncertainty propagation, is the Monte Carlo (MC) method. Typically the Monte Carlo algorithm allows uncertainty to

be propagated from inputs characterised by well-defined probability distribution functions (PDF) [17]. It is flexible, unbiased and one of the most well-established methodologies to propagate uncertainty, but its classical implementation does not differentiate between aleatory and epistemic uncertainty. This is a disadvantage from several points of view. First, it makes the analyst unable to grasp how much of the uncertainty is due to inherent variability and to what extent the uncertainty is due to poor data quality (therefore suitable to be reduced in principle). Secondly, it relies upon a good characterization of the variables to be sampled, which usually requires a considerable body of empirical information in order to properly define probability distributions. To overcome such limitations, more sophisticated MC algorithms can be used within generalised probabilistic frameworks to propagate both types of uncertainties without mixing them. For instance, the so-called double loop Monte Carlo algorithm [18] can be used. In this work, using classical probabilistic approaches the uncertain factors are described by probability distribution functions (PDFs) and a traditional MC approach is employed to propagate uncertainty. When generalised probabilistic approaches are adopted, parameters are characterised by P-boxes or DS structures and the uncertainty is propagated using the proposed double loop MC or Dempster-Shafer structures propagation algorithms (adopted as presented in Figure 1).

The double loop MC is presented by Figure 1-(a). A first loop (outer loop) samples from the epistemic uncertainty space $\Theta$. Each realisation corresponds to a classical probabilistic model for which only aleatory uncertainties must be considered. Then, a traditional MC simulation can be used (inner loop) to propagate aleatory uncertainty. The quantity $N_e$ is the number of realisations in the epistemic space and $N_a$ is the number of samples from the aleatory space. $\theta_j$ is the set of uncertain parameters of the epistemic space realizations $j$, sampled from a known set of intervals $[\underline{\theta}, \overline{\theta}]$. The quantity $x_{k,i}$ is the sample $i$ of the random variable $k$ obtained from the inverse transform of the associated CDF $F_{X_k|\theta_j}(x)$, which depends on the epistemic realization $\theta_j$. The cumulative distribution $F_{Y|\theta_j}(y)$ of the reliability performance $y$ can be used to compute $P_{f,j}$, which is the system failure probability given the epistemic realization $j$. The probability results of the inner loop are not to be averaged over the outer loop but only collected. Then the minimum and maximum can be selected to obtain bounds on the quantity of interest [19].

The Dempster-Shafer structures propagation procedure in Figure 1-(b), works as

follows:

1. First, $n$ "Parameter cells" are constructed by Cartesian product of the focal elements. Hence, each parameter cell $\omega$ is an hypercube $\omega : \{\underline{\mathbf{x}}_\omega \leq \mathbf{x} \leq \overline{\mathbf{x}}_\omega \; \forall \; \mathbf{x}\}$.
2. The minimum and maximum values of the system performance $y$ are calculated based on optimization technique and constrained by the $\omega$ bounds.
3. The $n$ resulting min-max intervals (i.e. propagation of the focal elements) are used to construct Dempster-Shafer structures.
4. Finally, Dempster-Shafer structures are converted to distribution-free P-boxes and the system reliability bounds $[\underline{P}_f, \overline{P}_f]$ obtained.

The computational cost of the procedure is proportional to the number of input intervals to be propagated and the time needed to simulate the system. Applicability for complex systems with highly non-regular behaviour, which are hence computationally expensive, can require a meta-modelling approach to speed-up the propagation procedure (e.g. Polynomial Chaos, Artificial Neural Networks).

OpenCossan [7] is a collection of methods and tools under continuous development at the Institute for Risk and Uncertainty, University of Liverpool, coded exploiting the object-oriented Matlab programming environment. It allows specialised solution sequences to be defined including a wide variety of reliability methods. Novel optimisation algorithms, reliability methods, and uncertainty quantification and propagation techniques can be easily integrated into the main software body. For these reasons, the developed methods (i.e. Algorithms in Figure 1) have been integrated into OpenCossan and adopted for the solution of two reliability assessments, see Sections 4.2 and 5. As a result of such development, OpenCossan can be used to perform uncertainty quantification adopting classical and generalised probabilistic methods.

## 4. Case Study I: The NAFEMS Challenge Problem

### *4.1. Problem Definition*

The challenge problem, prepared by the NAFEMS Stochastics Working Group [8], consists of four uncertainty quantification and information qualification tasks motivated by the need to promote best practices to deal with uncertainty to industry. The analysts are asked to evaluate the reliability of an electronic resistive, inductive, capacitive (RLC) series circuit. Four different cases (A, B, C and D) have been proposed

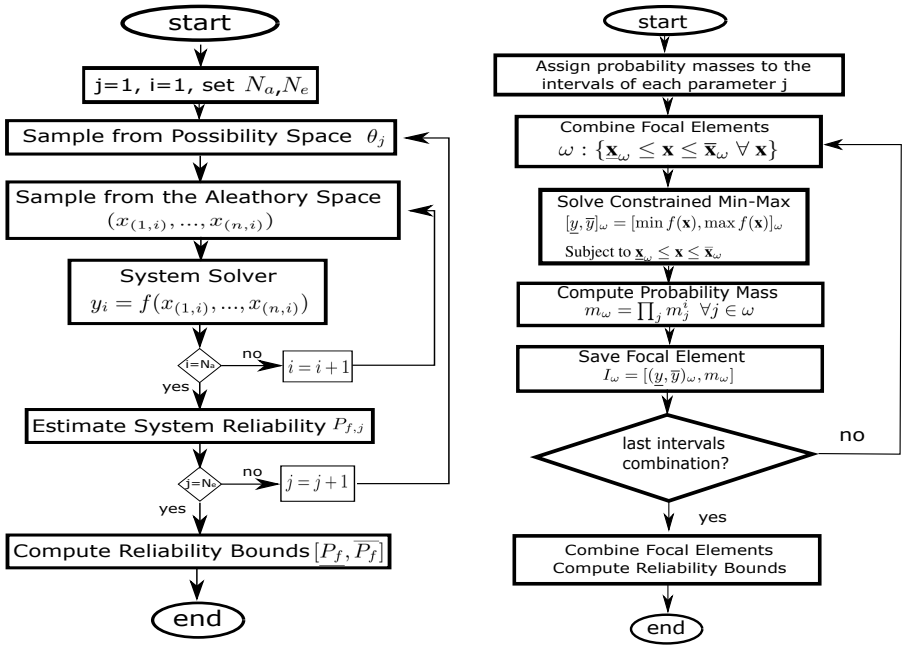


(a) Double loop Monte Carlo. (b) Dempster-Shafer structures propagation.

Figure 1: Flow charts for the double loop Monte Carlo (a) and the DS structures propagation (b).

in [8], each one having incomplete, scarce or imprecise information about the system parameters, as shown in Table 1. In CASE-A single intervals, i.e. one upper bound and one lower bound for parameter R, L and C are given. In CASE-B, each parameter can lay within multiple intervals, i.e. three upper and lower bounds. In CASE-C, ten sampled points for each parameter are provided. Finally, for CASE-D, imprecise bounds and nominal values is the only available information. The last case is similar to CASE-A, but one bound is not precisely defined. The equations governing the RLC circuit, although very simple, are provided by the challengers and reported here for completeness. The transfer function of the system is defined as:

$$\frac{V_c(t)}{V} = \frac{\omega^2}{S^2 + \frac{R}{L}S + \omega^2} \tag{2}$$

Depending on the values of R, L and C, the system may be classified as under-damped ($Z$ <1), critically damped ($Z$ =1) or over-damped ($Z$ >1) and having different solutions as detailed below.

Table 1: The available information for CASE-A, CASE-B, CASE-C, and CASE-D (data taken from[8]).

| CASE | R [$\Omega$] | L [mH] | C [$\mu$F] |
|---|---|---|---|
| A: Interval | [40,1000] | [1,10] | [1,10] |
| B: source 1 | [40,1000] | [1,10] | [1,10] |
| B: source 2 | [600,1200] | [10,100] | [1,10] |
| B: source 3 | [10,1500] | [4,8] | [0.5,4] |
| C: Samples | 861, 87, 430, 798, 219, 152, 64, 361, 224, 61 | 4.1, 8.8, 4.0, 7.6, 0.7, 3.9, 7.1, 5.9, 8.2, 5.1 | 9.0, 5.2, 3.8, 4.9, 2.9, 8.3, 7.7, 5.8, 10, 0.7 |
| D: Interval | [40,$R_{U1}$] | [1,$L_{U1}$] | [$C_{L1}$,10] |
| D: Other info | $R_{U1}$ >650 | $L_{U1}$ >6 | $C_{L1}$ <7 |
| D: Nominal Val. | 650 | 6 | 7 |

$$V_c(t) = \begin{cases} V + (A_1 cos(\omega t) + A_2 sin(\omega t)) \exp^{-\alpha t} & \text{if } Z < 1 \\ V + (A_1 + A_2 t) \exp^{-\alpha t} & \text{if } Z = 1 \\ V + (A_1 \exp^{S_1 t} + A_2 \exp^{S_2 t}) & \text{se } Z > 1 \end{cases} \quad (3)$$

Where $\alpha = \frac{R}{2L}$, $\omega = \frac{1}{\sqrt{LC}}$, the damping factor is $Z = \frac{\alpha}{\omega}$ and roots obtained as $S_{1,2} = -\alpha \pm \sqrt{\alpha^2 - \omega^2}$. Coefficients $A_1$ and $A_2$ are determined by assuming the initial voltage and voltage derivative equal zero and a unitary step voltage function is considered. In this case study, the main goals consist in qualifying the value of information and evaluating the reliability of the system with respect to three requirements:

$$V_c(t = 10ms) > 0.9\,V \;\;,\;\; t_r = t(V_c = 0.9V) \leq 8\;ms \;\;,\;\; Z \leq 1 \quad (4)$$

where $t_r$ is the voltage rise time, i.e. the time required to increase $V_c$ from 0 to 90% of the input voltage, and it has to be less than or equal 8 ms. The first two requirements are on the voltage at the capacitance $V_c$, the third requirement is on the damping factor, which assures that under-damped system responses are discharged ($Z \leq$1). Specifically, $V_c$(10ms), $V_c$(8ms) and $Z$ are regarded as performance variable for the system, and if these conditions are not satisfied the system is considered to have failed. Probabilistic and generalised probabilistic approaches are adopted to tackle the four cases and uncertainty characterization and propagation are presented for each case. Depending on the approach selected, CDFs or P-boxes are obtained for the three performance variables (see Eq.(4)). If $V_c$(10ms),$V_c$(8ms) and $Z$ result in crisp CDFs, the probability

of failure is computed by estimating the CDF values at 0.9 Volts for the requirements on $V_c$ and voltage rise time $t_r$ as well as the CDF value at $Z$=1 for the requirement on the damping factor. Similarly, if bounds on the CDFs are obtained (i.e. P-boxes), then bounds on probability of not meeting the requirements are computed as explained in Sections 2, which are $[\underline{P}_{Vc10}, \overline{P}_{Vc10}]$, $[\underline{P}_{tr}, \overline{P}_{tr}]$, and $[\underline{P}_{Z}, \overline{P}_{Z}]$, respectively. This case study was previously tackled by different groups and the author using different approaches. For further reading the reader is reminded to Refs. [8]-[20]. This work presents additional analyses of the NAFEMS challenge problem by adopting novel algorithms in a unified computational framework.

### *4.2. CASE-A and CASE-B*

In CASE-A, a single interval was provided for the parameters while multiple intervals were available in CASE-B (see, Table 1). CASE-B degenerates to CASE-A if the probability mass equal one is assigned to the first source of information. This because in CASE-B intervals values for source 1 corresponds to the interval values in CASE-A. Due to the considerations made, the two cases are presented and solved together.

*Probabilistic Approach*

In the CASE-A the intervals were propagated using a single loop Monte Carlo by assuming a uniform distribution within the bounds on R, L and C, which is an assumption made with respect to the principle of maximum entropy. The reliability is assessed by evaluating if the system requirements are met as shown in Eq. (4). For the solutions of CASE-A, failure probabilities have been estimated using $10^7$ samples and are $P_{Vc10}$ =0.243, $P_{tr}$ =0.345 and $P_Z$ =0.031. The probability of failure for requirement one is lower than the probability of failure for requirement two.

For the solution of the CASE-B, each interval is considered individually. Hence, three different uniform distributions for each R, L, and C parameter are used, one for each source of information. The reliability analyses have been performed to compute 3 probabilities of failure and results are shown in Table 2. The Source 3 has the lowest estimated probability of failure while the Source 1 shows an intermediate failure probability. On the right-hand side of Figure 2 the resulting CDFs for the three sources of information and three requirements are displayed.

Table 2: The results for CASE-B obtained by Monte Carlo method and $10^7$ samples.

| CASE-B | Source 1 | Source 2 | Source 3 |
|---|---|---|---|
| $P_{Vc10}$ | 0.243 | 0.549 | 0.052 |
| $P_{tr}$ | 0.340 | 0.660 | 0.129 |
| $P_Z$ | 0.031 | 1.25 $10^{-5}$ | 0.069 |

*Generalised Probabilistic Approach*

Possible values of the parameters (interval) can be represented by means of the generalised probabilistic approach without defining a probability distribution. Parameter uncertainty has been characterised using Dempster-Shafer structures. For CASE-A three Dempster-Shafer structures composed by a single focal element have been defined as $\left\{\underline{R_1}, \overline{R_1}], m_1\right\}$, $\left\{[\underline{L_1}, \overline{L_1}], m_1\right\}$ and $\left\{[\underline{C_1}, \overline{C_1}], m_1\right\}$, where the probability mass $m_1$ is equal one. For CASE-B, each DS structure is defined as:

$$\left\{([\underline{X_1}, \overline{X_1}], m_1), ([\underline{X_2}, \overline{X_2}], m_2), ([\underline{X_3}, \overline{X_3}], m_3)\right\}$$

where $[\underline{X_i}, \overline{X_i}]$ represents the $i^{th}$ interval source for one of the parameters (R, L or C) and $m_i$ is the associated probability mass. The CASE-B degenerate to the CASE-A if the probability mass $m_2$ and $m_3$ are set equal to zero. It was not possible here to establish if some sources of information are better, thus, pieces of information derived from different sources are assumed as equally likely, i.e. $m_1 = m_2 = m_3 = 1/3$. Twenty-seven parameter cells are constructed by the permutation of the intervals. Then, minimizations and maximisations of $V_c$(8ms), $V_c$(10ms) and $Z$ were performed to identify the bounds of the system performance. The output Dempster-Shafer structures are used to create probability boxes for the system performances $V_c$(8ms), $V_c$(10ms) and $Z$ and the corresponding failure probabilities obtained.

Applying the procedure to the CASE-A, the resulting P-boxes give no valuable information on the failure probability for the three performance requirements. The probability of failure is in fact just bounded in the interval [0,1] for all the requirements. The CASE-B includes all the information available for the CASE-A plus two additional sources of information. The additional intervals contribute to reducing the uncertainty on the system performance as shown on the right-hand side of Figure 2. Resulting bounds are also presented in Table 3 and it can be noticed that the outputs have high associated uncertainty, but less than that in the CASE-A. $P_{tr}$ lays within the interval

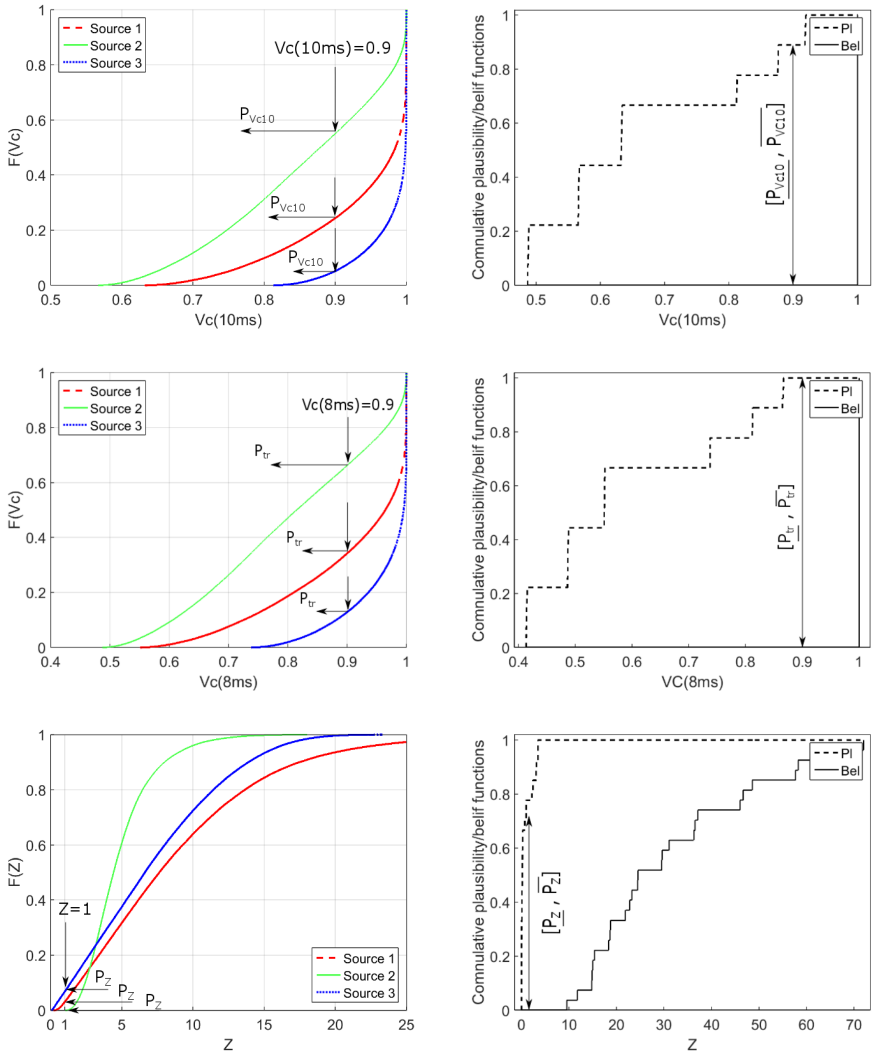


Figure 2: Comparison of the $V_c(8ms)$,$V_c(10ms)$ and $Z$ results for CASE-B, respectively. Resulting CDFs obtained using the probabilistic approach (on the left) and P-boxes obtained from the generalised approach (on the right).

[0,0.9], $P_{Vc10}$ within [0,1] and $P_Z$ lays within the interval [0,0.7]. Hence, failure probability for requirement two does not show any reduction in the uncertainty.

The failure probability computed by adopting classical approaches always lays within the bounds obtained using the Dempster-Shafer methodology, as shown in Figure 2. The maximum failure probability for the Z requirement is 0.069 (source 3), while the

Table 3: The results of CASE-B obtained adopting generalised probabilistic approach.

| CASE-B | Source 1 | Source 2 | Source 3 | All Sources |
|---|---|---|---|---|
| $P_{Vc10}$ | [0,1] | [0,1] | [0,1] | [0,0.9] |
| $P_{tr}$ | [0,1] | [0,1] | [0,1] | [0,1] |
| $P_Z$ | [0,1] | [0,1] | [0,1] | [0,0.7] |

generalised approach bounds the results between 0 and 0.7. This reliability overestimation was due to the assumption made on the parent distribution needed to apply the classical methodology. In fact, by selecting a PDF we explicitly assume a well-defined stochastic behaviour for the parameters. As a matter of fact, no information was given to assume a random behaviour at all, and the imprecise information could be due to different experts advising for different scale ranges to be analysed.

The computational time for CASE-B using classical Monte Carlo simulation was about 6.7 seconds. The generalised solution to CASE-A and CASE-B was relatively computationally inexpensive, taking about 0.07-0.08 seconds for the solution of each min-max problem. Thus, the DS structures propagation for the 3 reliability requirements took just 5-6 seconds for CASE-B on a 4 cores machine with 8.00 Gb ram and a 2.00 GHz Intel® Core™ i5-4590T processor.

### *4.3. CASE-C*

*Probabilistic Approach*

For the solution of CASE-C, two methodologies were adopted. Firstly a uniform distribution approach and secondly a Kernel Density estimation (KDE) approach [15]. The uniform distribution approach allows the values of the parameters to change within the sampled range (but not outside). The bounds are assumed equal to the minimum and maximum values of the samples. Then, $10^5$ MC run have been performed obtaining estimated probabilities of failure of $P_{Vc10}$=0.183, $P_{tr}$=0.273, $P_Z$=0.016, respectively. The Kernel Density Estimator is a well-known approach that allows a probability distribution to be constructed based on sample data without assuming its distribution form. Different Kernels can be used and the Gaussian Kernel is a popular choice which has been adopted in this work because it allows the incorporation of measurement error. The optimal bandwidth value was obtained using Silverman's rule of thumb [15]. By adopting KDE the estimated failure probabilities are $P_{Vc10}$=0.232,

$P_{tr}$=0.292, $P_Z$=0.121, respectively. These values are slightly larger compared to the one obtained with the uniform distribution approach. Higher values of the probability of failure are due to the tails of the Kernel fitted probability distribution (displayed in Figure 3) which allows the value of the parameter to change outside the range of the samples. Plots on the left-hand side in Figure 4 show the output CDFs when adopting uniform distributions and KDE to model parameter uncertainty. The CDF of $Z$ has been zoomed around the value $Z$=1 for graphical reasons. The failure probabilities calculated using sampled values of R, L and C are also lower if compared to the ones obtained in CASE-A and CASE-B. This is due to the smaller upper bound on R in CASE-C (861 Ohm).

*Generalised Probabilistic Approach*

CASE-C is solved by applying the Kolmogorov-Smirnov (KS) test to characterise the uncertainty of the input parameters as shown in [14], and obtaining bounds on the empirical cumulative probability distribution function. Maximum and minimum values of the parameters are assumed and the CDF upper and lower bounds are truncated accordingly. Due to the underlying physics governing the system, all the parameters must be positive and this condition allows the lower bounds to be set. Truncating the tails of the distributions, especially in reliability analysis, can lead to erroneous results and safety overconfidence. Thus a relatively high upper bound for the CDF truncation was selected, which was assumed equal to the sample mean plus three times the sample's standard deviation. In Figure 3 the upper and lower bounds (dashed and solid lines) are shown for the empirical CDF (square marker blue line) and the Kernel density estimator (blue dot-dashed line). Three different confidence levels for the KS test are used for each parameter. The bounds on the left-hand side plots refer to a confidence level $\alpha$=0.05 and they are compared to the plots on the right-hand side which show the obtained bounds for $\alpha$=0.01 (dashed and solid star marker lines), $\alpha$=0.1 (dashed and solid blue lines) and $\alpha$=0.2 (dashed and solid circle marker lines).

The obtained P-boxes are propagated through the system. On the right plots of Figure 4, the voltage at the $10^{th}$ ms, $8^{th}$ ms and damping factor P-boxes are presented, red blue and black colour lines with different markers refer to confidence level $\alpha$=0.01, $\alpha$=0.1 and $\alpha$=0.2 respectively. The P-box of the damping factor has been zoomed around the value $Z$=1 to improve the readability of the plot. The bounds on the probabilities of failure are presented in the Table 4. It can be observed that the intervals

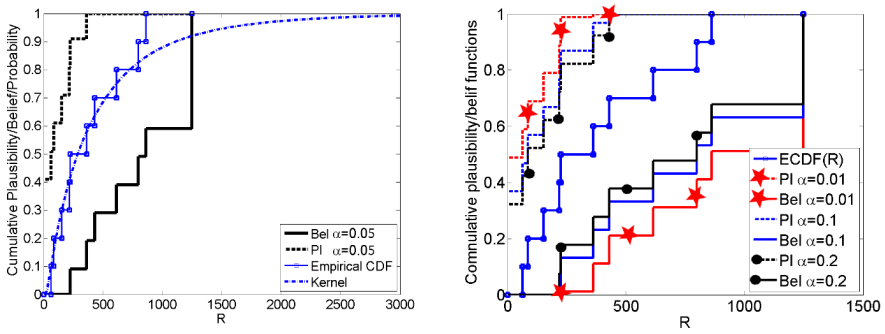


Figure 3: The Kernel fitting (on the right panel) and the P-box bounds (on the right panel) of the resistance R for the CASE-C.

Table 4: The results for CASE-C, the probability bounds for the three requirements and the three confidence levels.

| CASE-C | $\alpha$=0.01 | $\alpha$=0.1 | $\alpha$=0.2 |
|---|---|---|---|
| $P_{Vc10}$ | [0,0.87] | [0,0.7] | [0,0.63] |
| $P_{tr}$ | [0,0.92] | [0,0.77] | [0,0.7] |
| $P_Z$ | [0,0.83] | [0,0.7] | [0,0.64] |

on the failure probability are quite wide, as already observed for CASE-A and CASE-B. Nevertheless, the failure probability bounds appear to be narrower if compared to CASE-A and CASE-B. This shows that the information provided for CASE-C is of higher quality, which allows less imprecise reliability estimates to be obtained. The results show that the uncertainty in the system reliability was underestimated by using the Monte Carlo method because precise probability distribution functions were assumed despite the small sample size. The failure probabilities estimated by adopting the classical approach lay within the probability interval obtained by adopting generalised approaches.

Using the same machine adopted for solving the previous cases, the classical probabilistic solution of CASE-C required about 0.07 seconds for the fitting and propagation of the Kernel probability densities and additional 0.05 seconds for the propagation of uniform probability densities. Conversely to the generalised solution to CASE-A and CASE-B, the computational time needed for the propagation of the focal elements is generally higher when compared to its classical probabilistic counterpart. The DS

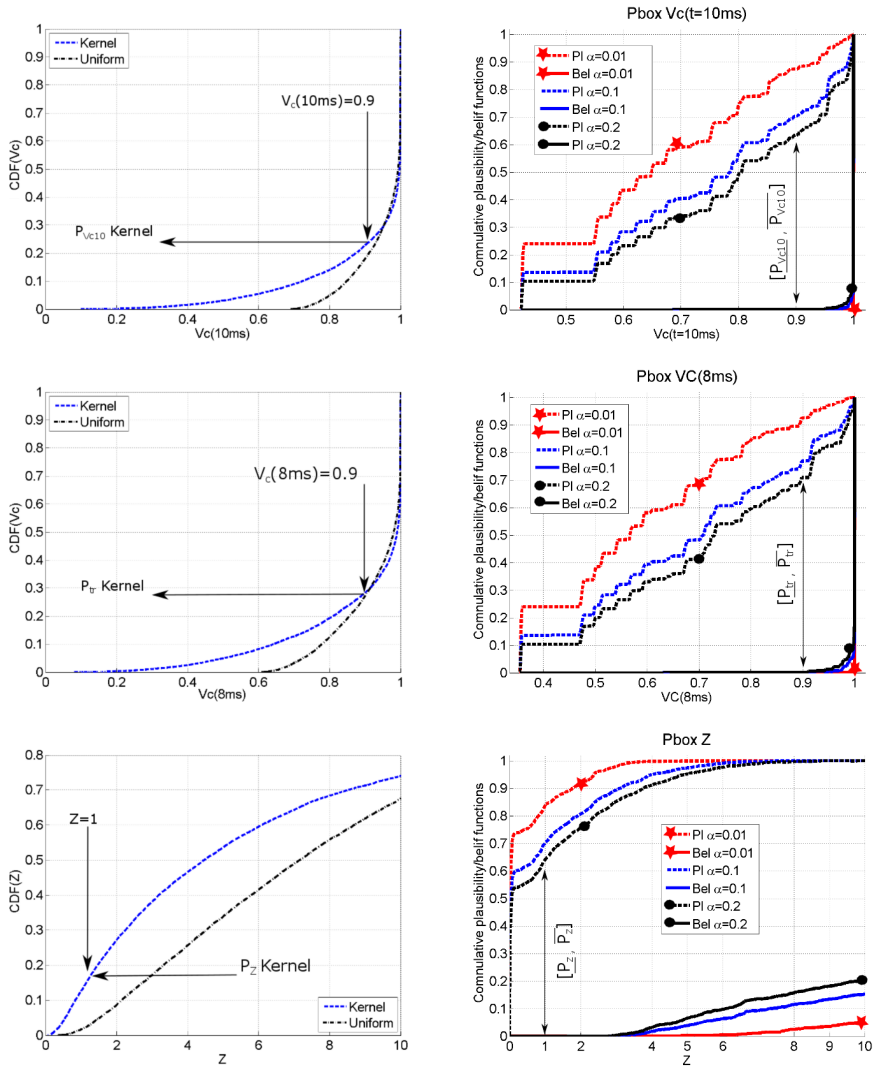


Figure 4: CDFs (on the left pannel) and P-boxes (on the right pannel) of $V_c$(10ms), $V_c$(8ms) and Z for the CASE-C

structures propagation took about 461 seconds for each confidence level $\alpha$ (i.e. about 23 minutes for the 3 confidence levels). The higher computational cost is attributable to the larger number of min-max optimisations performed (i.e. 2197 combinations of focal elements).

### *4.4. CASE-D*

Similarly to CASE-A, the bounds of the parameters are provided. However, just one bound is precisely defined for each parameter. The upper bounds of R and L and the lower bounds of C are imprecisely defined as shown in the last row of Table 1. In addition, the nominal values for the parameter are provided. The problem has been tackled by defining upper bounds of R and L, which were redefined as $T$ times their nominal value while the lower bound of C was redefined as its nominal value divided by $T$, where $T$ =10. Thus, the maximum truncation bounds are $\overline{R}_n$=6500 Ω, $\overline{L}_n$=60 mH and $\underline{C}_n$=0.7$\mu$F. The quantity $T$ is defined as 'truncation level' and $n$ =10 linearly spaced intermediate bounds are also considered.

*Probabilistic Approach*

Uniform PDFs are assumed within the defined intervals and all combinations of upper and lower bounds are propagated by the Monte Carlo method. Having reduced the semi-definite intervals to a set of defined intervals, it is now possible to estimate the reliability of the systems by adopting the same approach as CASE-B. For the first two requirements, the probability of failure increases from 0.1 up to 0.9. The MC method is not efficient in providing solutions for the lower bounds of the intervals. In fact, the probability of having $Z$ <1 goes from a maximum of 0.2 to a minimum of approximatively 0.0005 (requiring at least $10^5$ samples for a rough estimation).

*Generalised Probabilistic Approach*

The parameters' uncertainty has been characterised using a set of $n$ multiple intervals translated into DS structures. A probability mass function equal to $1/n$ has been assigned to each interval (for normalization reasons) defining Dempster-Shafter structures for the parameters, for instance the structure of R is $\left\{([\underline{R}, \overline{R}_1], \frac{1}{n}), ..., ([\underline{R}, \overline{R}_n], \frac{1}{n})\right\}$. The three probabilities of failure lay within the interval [0,1]. In particular, the imprecision associated with the last requirement indicates a severe misjudgement of the real uncertainty when the only classical probabilistic solution is considered (obtaining a maximum $P_Z$ =0.2). In order to investigate the effect of the assumptions on the results, a sensitivity analysis of the values of $\overline{R}_n$, $\overline{L}_n$ and $\underline{C}_n$ is performed. The sensitivity approach adopted is similar to the one-at-a-time method presented in [21]. The selected base-case has truncation level $T$=10 and truncation bounds $\overline{R}_n$=6500 Ω, $\overline{L}_n$=60 mH and $\underline{C}_n$=0.7$\mu$F. A total of 27 sensitivity cases are defined by selecting 9

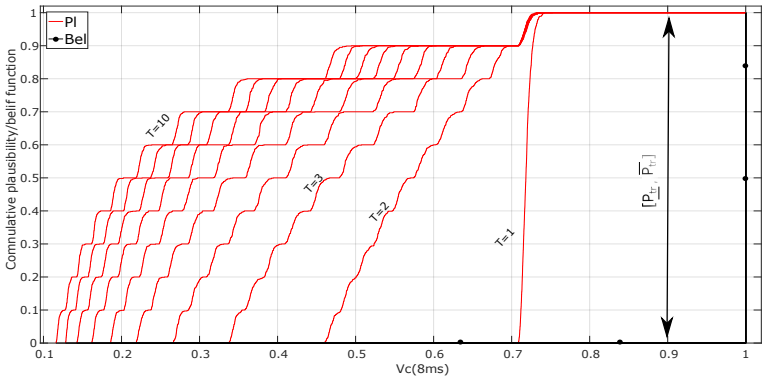


Figure 5: Variation in the probability bounds due different values of $\overline{R}_n$. The truncation values are $\overline{R}_n$=650·$T$ Ω with $T$=1,..,10 and $\overline{L}_n$=60 mH and $\underline{C}_n$=0.7$\mu$F.

truncation level to $T$=9,8,7..,1 for each one of the parameters taken one-at-a-time. Then uncertainty propagation is carried out for the sensitivity cases and results compared to the bounds of the base case. The comparison shows that the shape of the P-boxes is affected most by $\overline{R}_n$. On the other hand, it does not have relevant effects on the bounds of the failure probability. Figure 5 displays the sensitivity analysis performed by varying $\overline{R}_n$.

The computational time required to solve CASE-D is about 200 seconds by using the DS structure propagation algorithm whilst the classical approach required 1400 seconds for the solution (selecting $10^5$ samples for the Mone Carlo and propagating all the combinations of upper and lower bounds).

## 5. Case Study II: Analysis of a Power Transmission Network

The case study selected for the analysis is a 6-bus and 11-lines power transmission network [22]. Figure 6 displays the network topology, nodes indices and load names. The nodes 1-3 represent the generator buses while the nodes 4-6 are the demand buses. To simplify the reliability assessment, loads correlation is neglected and grid stress is increased. The reference loads $L_{d4}$, $L_{d5}$ and $L_{d6}$ and the decreased maximum power capacity of the generators are reported in Figure 6.

It is assumed that a lack of data is affecting the failure rate of the transmission lines. This is a common situation for highly reliable components for which at best only a few failures have been observed. A common practice used to estimate the failure rate of

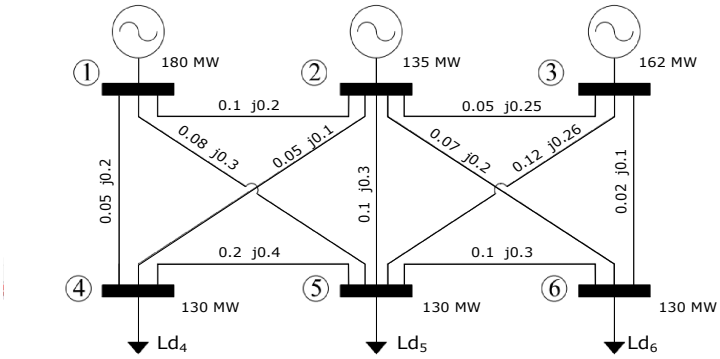


Figure 6: The 6-bus power network system.

transmission lines is to merge the few available failure samples between similar lines. This procedure is named "data pooling" and assumes that the behaviour of similar components can be described by the same probabilistic model. This is often a rational assumption. However, when (similar) components are subjected to different work loads (e.g. close/far from their thermal limits), different conditions (e.g. in a harsh/mild environment) or with different maintenance policies such assumptions are rarely true. Different endogenous and operational-environmental factors will most likely influence the ageing of the components and produce a very different failure behaviour even for identical lines. For more details on the problem, the reader is referred to [23].

The transmission links in the system are assumed to be LGJ-300 and for this specific line, an estimation of the failure rates ($\lambda_l$) for each link $l$ is presented in [24]. The available data consists of 40 failure times collected over 10 years for a first line and 5 years of failure times for a second. Over the first 5 years, the estimated $\lambda_l$ is 0.00027 [failure/h] while for the last 3 years the failure rate increases to 0.00042 [failure/h] (possibly due to a poorly described ageing effect). Similarly to CASE-A in the first case study (Section 4), an interval data source is considered for each line failure rate $\lambda_l$ with $l = 1, .., 11$. The failure rate is imprecisely defined during the ageing of the line (e.g. between 5 years to 8 years from installation) and this might affect the estimation of the power network reliability.

The Energy-not-Supplied (ENS) is a well-known reliability indicator for power grids and is employed here to assess the network failure probability. The power network is

simulated for a given period of time (e.g. 1 day) and random components' failures are sampled from probability distributions used to model the components' failure times. The probability of failure for a line is assumed to follow a Poison distribution and obtained similarly to [2]. During the simulation, the network power flow equations are solved and in the case of occurred failures or unsatisfied constraints (e.g. thermal or generators capacity limits), part of the power load can be curtailed. The power grid will fail to meet the performance requirement if the energy not provided to the customers is larger than a predefined threshold level (i.e. $ENS > ENS_{tsh}$). The $ENS_{tsh}$ has been set equal to 0.05 $\%$ of the total load demand. Further details on the reliability model are available in Ref. [25]. First, a classical probabilistic approach is used to assess the power grid reliability. The probabilistic model for the grid has to be precisely defined. Hence, a point value for the failure rate of each ageing line has been selected and set equal to the mean failure rate (0.000345 [outage/years]). A plain Monte Carlo is employed to propagate $10^4$ independent realisations of the power grid history. In each MC run, failures can randomly occur according to the line failure probability and the $ENS$ is computed for the sampled network state. The resulting CDF of the Energy-Not-Supplied ($F_{ENS}$) is displayed by the blue circle markers line in Figure 7. It can be used to obtain the probability of failure for the network as follows: $P(ENS > ENS_{tsh}) = 1 - F_{ENS}(ENS_{tsh})$.

The imprecise information available for the failure rate has been propagated using a

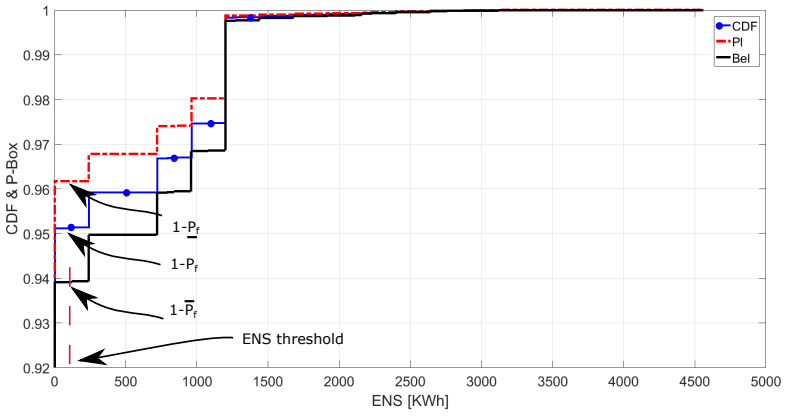


Figure 7: The CDF, Cumulative belief and Cumulative plausibility functions for the $ENS$ in [MWh]. The plot is zoomed in to better display the reliability results and $ENS_{tsh}$.

Table 5: The probability bounds resulting from the generalised approach accounting for 4 levels of imprecision for the nodal load demand, $L_{di}$.

| Imprecision on $L_{di}$ | 5% | 10% | 15% | 20% |
|---|---|---|---|---|
| $\overline{P}_f$ | 0.0874 | 0.0964 | 0.0964 | 1 |
| $\underline{P}_f$ | 0.0389 | 0.0387 | 0.0384 | 0.032 |

double loop Monte Carlo approach as presented in Section 3. In the outer loop, 50 values of the failure rates are sampled from the interval [0.00027,0.00042] failure/h and forwarded to the inner loop. In the inner loop, analogously to the classical probabilistic analysis, a Monte Carlo simulation is used to obtain independent histories for the power network, sampling failed components and obtaining the $ENS$. The results are cumulative belief (black solid line) and plausibility (dot-dashed red line), displayed in Figure 7. The threshold $ENS_{tsh}$ is also presented with a dashed line. The resulting reliability interval is [3.89, 6.09]$\cdot 10^{-2}$ which includes the single-valued reliability estimator obtained by the classical probabilistic approach, 4.99$\cdot 10^{-2}$.

The analysis has been extended by accounting for imprecision in the power loads $L_{d4}$, $L_{d5}$ and $L_{d6}$. In Ref. [26], power demand is affected by imprecision and modelled using two interval cases. Similarly, 4 imprecision levels on the power demanded (from 5% to 20% of the design load) are considered here, due for instance to measurement errors or forecast incertitude. Table 5 summarises the result for increasing imprecision on the load value and Figure 8 displays the output cumulative $Pl$ and $Bel$. The reliability bound gets wider the larger the imprecision surrounding the system loads is. It is worth noticing that when the load interval is increased from 15 to 20 % the upper failure probability increases drastically, from 9.64$\cdot 10^{-2}$ to 1 (dashed marked lines in Figure 8). This because within the parameter cell $\omega : \left\{\underline{L}_{di} \leq L_{di} \leq \overline{L}_{di} \; \forall \; i = 4, 5, 6\right\}$ exists at least one combinations of loads $(L_{d4}, L_{d5}, L_{d6})$ for which the power flow can not satisfy the given constraints (i.e. power balance, thermal limit and generators capacity constraints). As consequence, the power flow solver curtails a significant amount of load even for undamaged grid conditions and for each realisation within the inner loop the $ENS$ exceeds $ENS_{tsh}$.

In this final application, the developed framework has been tested using a more complex engineering application. Comparing the results obtained using the classical and generalised probabilistic approaches helped to understand the quality of the informa-

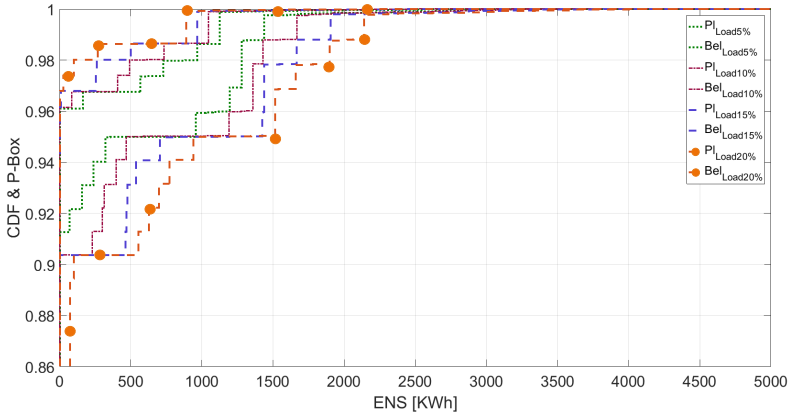


Figure 8: The Cumulative belief and plausibility functions for different levels of imprecision on the loads. The plot is zoomed in to improve the graphical output.

tion on $\lambda_l$ and loads and their impact on the network reliability. In the first case, the information quality was good and the imprecise data resulted in a moderate (but definitely observable) effect on the network reliability. In the second analysis, an increasing level of imprecision affecting the power demand is considered. The results showed that more imprecision in the input load increases the imprecision in the reliability estimate. Moreover, the generalised approach pointed out that increasing the imprecision in the load up to $20\%$, drastically stretched the reliability bounds (about [0,1]). This is indeed an indicator of a severe lack of the available information quality, which has been successfully pointed out by the generalised approach. The computational time for the solution was about 98 seconds using classical approaches (MC with $10^4$ samples) and about 4900 seconds for the generalised approach (50 outer loop samples and $10^4$ inner loop samples).

## 6. Limitation Faced and Discussions

Classical probabilistic approaches require the estimation of (or assuming) PDFs to describe parameters. Uncertainty and uniform distributions and Kernel density estimators have been used to characterise parameter uncertainty. In both cases, it has been explicitly assumed that the analysed parameters have some sort of stochastic nature, which in reality might not be true. One of the strongest limitations of classical probabilistic approaches is the need to represent the epistemic uncertainty as aleatory and

then mix these two types of uncertainty. The analysed NAFEMS reliability problem has confirmed that artificial model assumptions might lead to an underestimation of the uncertainty. Hence the reliability analysis might not represent precisely the real quality of the available data. For extreme cases, a severe lack of data can lead to non-informative bounds [0,1]. The large epistemic uncertainty about the system parameters may suggest considering an investment in collecting more empirical data rather than refining the model for the reliability assessment. The overall outcomes of the study highlighted some of the positive and negative aspects of employ a generalised approach with respect to classical uncertainty quantification methodologies.

The reliability assessments were affected by severe uncertainty when, if tackled using classical probabilistic approaches, the analyst is forced to make unjustified assumptions leading to a strong underestimation the true output uncertainty. A case affected by a severe lack of data was the NAFEMS reliability problem for which the epistemic component appeared to be a dominant part of the outcomes' uncertainty. On the other hand, a reliability problem affected by a mild lack of data would have had results less sensitive to the epistemic uncertainty. This might be well-represented by the power grid reliability problem for which the failure rate imprecision influenced moderately (but visibly) the precision of reliability estimate. Similar results have been obtained for imprecision on the load demand up to 15 $\%$. On the other hand, higher imprecision on the load ($20\%$) drastically widened the reliability bounds. This has been pointed out thanks to the proposed comparison framework for classical and generalised probabilistic approaches.

## 7. Conclusions

In order to define a precise and 'exact' probabilistic model, a very high amount of data (possibly infinite) would be necessary. Unfortunately, a lack of information always affects engineering analysis and its extent cannot be quantified a priori. In general, the quality of the available information is context and scope-dependent, e.g. different systems performance indicators may react very differently to the same lack of data. The proposed framework provides a simple but effective way to assess a data deficiency by comparing the system reliability bounds (obtained through generalised probabilistic approaches) against single-valued probability indicators (obtained adopting classical probabilistic methods). If the lack of knowledge is mild, the system reliability will result in relatively narrow bounds which include the point reliability estimator. In this

case, classical approaches will be well-suited to tackle the problem. Otherwise, the lack of data will be severe and reliability bounds wide or, for extreme cases, even non-informative ([0,1]). Combination of pure probabilistic approaches (e.g. Monte Carlo Simulation) and generalised uncertainty quantification approaches (e.g. based on Dempster-Shafer structures and probability boxes), implemented in a common computational framework, are unavoidable tools for the industry which may rely on multiple accurate information qualification approaches. This will aid understanding if the data is of high quality or poor quality, with the aim of designing safer and more reliable systems and components. The NAFEMS uncertainty quantification challenge problem and a power system reliability assessment have been selected as representative test cases and have been solved using the proposed computational tool. Essential information has been provided and the quality of the available data assessed.

## References


[1] M. Beer, E. Patelli, Editorial: Engineering analysis with vague and imprecise information, Structural Safety 52, Part B (0) (2015) 143, engineering Analyses with Vague and Imprecise Information. doi:http://dx.doi.org/10.1016/j.strusafe.2014.11.001.

[2] R. Rocchetta, Y. Li, E. Zio, Risk assessment and risk-cost optimization of distributed power generation systems considering extreme weather conditions, Reliability Engineering & System Safety 136 (0) (2015) 47 – 61. doi:http://dx.doi.org/10.1016/j.ress.2014.11.013.

[3] Y. Z. Ma, P. R. La Pointe (Eds.), Uncertainty Analysis and Reservoir Modeling, American Association of Petroleum Geologists, 2011. doi:10.1306/M961330.
URL http://geoscienceworld.org/content/9781629810102/9781629810102

[4] A. Hot, T. Weisser, S. Cogan, An info-gap application to robust design of a prestressed space structure under epistemic uncertainties, Mechanical Systems and Signal Processing 91 (Supplement C) (2017) 1 – 9.

[5] S. Ferson, Estimating rare-event probabilities without data., in: Proceedings of the 12th International Conference on Structural Safety & Reliability (ICOSSAR), 2017, Wien, Austria, p. 1.

[6] M. Beer, S. Ferson, V. Kreinovich, Imprecise probabilities in engineering analyses, Mechanical Systems and Signal Processing 37 (12) (2013) 4 – 29.

[7] E. Patelli, Cossan: A multidisciplinary software suite for uncertainty quantification and risk management, in: R. Ghanem, D. Higdon, H. Owhadi (Eds.), Handbook of Uncertainty Quantification, Springer International Publishing, Cham, 2016, pp. 1–69.

[8] M. Fortier, R. Rebba, P. Koch, A. Karl, M. Broggi, L. Wright, Challenge in uncertainty quantification, Bench Mark, The International Magazine for Engineering Designers & Analysis from NAFEMS, Medical Modelling (2014) 40–43.

[9] G. Shafer, A Mathematical Theory of Evidence, Princeton University Press, Princeton, 1976.

[10] T. Augustin, Optimal decisions under complex uncertainty - basic notions and a general algorithm for data-based decision making with partial prior knowledge described by interval probability, Special Issue of ZAMM - Zeitschrift fr Angewandte Mathematik und Mechanik 84 (10–11) (2004) 1–10.

[11] P. Verma, P. Singh, K. George, H. Singh, S. Devotta, R. Singh, Uncertainty analysis of transport of water and pesticide in an unsaturated layered soil profile using fuzzy set theory, Applied Mathematical Modelling 33 (2) (2009) 770 – 782.

[12] Y. Ben-Haim, Robust rationality and decisions under severe uncertainty, Journal of the Franklin Institute 337 (23) (2000) 171 – 199.

[13] E. Patelli, D. Alvarez, M. Broggi, M. De Angelis, Uncertainty management in multidisciplinary design of critical safety systems, Journal of Aerospace Information Systems 12 (1) (2015) 140–169, cited By 3. doi:10.2514/1.I010273.
URL https://www.scopus.com/inward/record.uri?eid=2-s2.0-84922432517&doi=10.2514%2f1.I010273&partnerID=40&md5=692dfe1597398e379caaad3735476d61

[14] S. Ferson, V. Kreinovich, L. Ginzburg, D. S. Myers, K. Sentz, Constructing probability boxes and Dempster-Shafer structures, Vol. 835, Report SAND2002-4015, Sandia National Laboratories, Albuquerque, NM, 2003.

[15] H. Pradlwarter, G. Schuëller, The use of kernel densities and confidence intervals to cope with insufficient data in validation experiments, Computer Methods in Applied Mechanics and Engineering 197 (2932) (2008) 2550 – 2560, validation Challenge Workshop.

[16] A. P. Dempster, A Generalization of Bayesian Inference, Springer Berlin Heidelberg, Berlin, Heidelberg, 2008, pp. 73–104. doi:10.1007/978-3-540-44792-4_4.
URL https://doi.org/10.1007/978-3-540-44792-4_4

[17] M. Marseguerra, E. Zio, Basics of the Monte Carlo Method with Application to System Reliability, LiLoLe - Verlag GmbH (Publ. Co. Ltd.), Hagen, Germany, 2002, iSBN 3-934447-06-6.

[18] T. Ali, H. Boruah, P. Dutta, Modeling uncertainty in risk assessment using double monte carlo method, International Journal of Engineering and Innovative Technology 1 (4) (2012) 114–118.

[19] M. Sallak, W. Schon, F. Aguirre, Extended component importance measures considering aleatory and epistemic uncertainties, IEEE Transactions on Reliability 62 (1) (2013) 49–65. doi:10.1109/TR.2013.2240888.

[20] R. Rocchetta, E. Patelli, M. Broggi, S. Schewe, Robust probabilistic risk/safety analysis of complex systems and critical infrastructures, Master of Research in Decision Making Under Risk and Uncertainty, Liverpool University, 2015.

[21] E. Borgonovo, E. Plischke, Sensitivity analysis: A review of recent advances, European Journal of Operational Research 248 (3) (2016) 869 – 887. doi:http://dx.doi.org/10.1016/j.ejor.2015.06.032.

[22] A. J. Wood, B. F. Wollenberg, Power Generation, Operation, and Control, 2nd Edition, pp. 104, 112, 119, 123-124, 549, ohn Wiley & Sons, NY, Jan 1996.

[23] A. Moradkhani, M. R. Haghifam, M. Mohammadzadeh, Failure rate estimation of overhead electric distribution lines considering data deficiency and population variability, International Transactions on Electrical Energy Systems 25 (8) (2015) 1452–1465, eTEP-13-0523.R2.

[24] M. Yang, J. Wang, H. Diao, J. Qi, X. Han, Interval estimation for conditional failure rates of transmission lines with limited samples, IEEE Transactions on Smart Grid PP (99) (2016) 1–1. doi:10.1109/TSG.2016.2618623.

[25] R. Mena, M. Hennebel, Y.-F. Li, C. Ruiz, E. Zio, A risk-based simulation and multi-objective optimization framework for the integration of distributed renewable generation and storage, Renewable and Sustainable Energy Reviews 37 (2014) 778 – 793.

[26] L. V. Barboza, G. P. Dimuro, R. H. S. Reiser, Towards interval analysis of the load uncertainty in power electric systems, in: 8th International Conference on Probabilistic Methods Applied to Power Systems, 2004, pp. 538–544.